

## LETTERS

# Chaos in a long-term experiment with a plankton community

Elisa Benincà<sup>1,2\*</sup>, Jef Huisman<sup>1\*</sup>, Reinhard Heerkloss<sup>3</sup>, Klaus D. Jöhnk<sup>1†</sup>, Pedro Branco<sup>1</sup>, Egbert H. Van Nes<sup>2</sup>, Marten Scheffer<sup>2</sup> & Stephen P. Ellner<sup>4</sup>

Mathematical models predict that species interactions such as competition and predation can generate chaos<sup>1–8</sup>. However, experimental demonstrations of chaos in ecology are scarce, and have been limited to simple laboratory systems with a short duration and artificial species combinations<sup>9–12</sup>. Here, we present the first experimental demonstration of chaos in a long-term experiment with a complex food web. Our food web was isolated from the Baltic Sea, and consisted of bacteria, several phytoplankton species, herbivorous and predatory zooplankton species, and detritivores. The food web was cultured in a laboratory mesocosm, and sampled twice a week for more than 2,300 days. Despite constant external conditions, the species abundances showed striking fluctuations over several orders of magnitude. These fluctuations displayed a variety of different periodicities, which could be attributed to different species interactions in the food web. The population dynamics were characterized by positive Lyapunov exponents of similar magnitude for each species. Predictability was limited to a time horizon of 15–30 days, only slightly longer than the local weather forecast. Hence, our results demonstrate that species interactions in food webs can generate chaos. This implies that stability is not required for the persistence of complex food webs, and that the long-term prediction of species abundances can be fundamentally impossible.

The discovery by May in the 1970s that simple population models may generate complex chaotic dynamics<sup>1,2</sup> triggered heated debate and caused a paradigm shift in ecology. Since May's findings, mathematical models have shown that chaos can be generated by a plethora of ecological mechanisms, including competition for limiting resources<sup>6,8</sup>, predator–prey interactions<sup>3,5</sup> and food-chain dynamics<sup>4,7</sup>. In contrast to the overwhelming theoretical attention, convincing empirical evidence of chaos in real ecosystems is rare<sup>13</sup>. What could explain the paucity of empirical support? It might be that chaos is a rare phenomenon in natural ecosystems, for instance because food webs contain many weak links between species, which may stabilize food-web dynamics<sup>14,15</sup>. Alternatively, one might argue that there is a lack of suitable data to test for chaos in food webs. For instance, external variability (for example, weather fluctuations) may obscure the role of intrinsic species interactions. In principle, laboratory experiments provide ideal conditions to obtain high-resolution data in a constant environment. Chaos has so far been demonstrated experimentally for a few single species<sup>9,10</sup>, a three-species food web<sup>11</sup> and nitrifying bacteria in a wastewater bioreactor<sup>12</sup>. Thus far, however, laboratory studies have not considered the natural complexity of real food webs, and the time span of experiments has often been too short to detect chaos in a rigorous manner.

Here, we analyse a time series of a plankton community isolated from the Baltic Sea. The plankton community was cultured in a laboratory mesocosm under constant external conditions for more than eight years<sup>16</sup>. In total, two nutrients (nitrogen and phosphorus), one detritus pool and ten different functional groups were distinguished (Fig. 1a). The phytoplankton was divided into picophytoplankton, nanophytoplankton and filamentous diatoms. The herbivorous zooplankton was classified into protozoa, rotifers and calanoid copepods. The rotifers and protozoa were grazed by cyclopoid copepods. The microbial loop was represented by heterotrophic bacteria and two groups of detritivores: ostracods and harpacticoid copepods. The abundances of these functional groups were counted twice a week. Our analysis covers a period of 2,319 days, which yielded 690 data points per functional group. Because most species in this food web have generation times of only a few days, the time series spanned hundreds to thousands of generations per species. We performed several analyses to investigate the dynamics of this food web.

First, the time series showed fluctuations in species abundances over several orders of magnitude, despite constant external conditions (Fig. 1). Spectral analysis revealed that the fluctuations covered a range of different periodicities (see Supplementary Information). In particular, picophytoplankton, rotifers and calanoid copepods seemed to fluctuate predominantly with a periodicity of about 30 days, suggestive of coupled phytoplankton–zooplankton oscillations. Periodicities of about 30 days are consistent with model predictions of phytoplankton–zooplankton oscillations<sup>17</sup>, and have been observed in earlier laboratory experiments with phytoplankton and zooplankton species<sup>18</sup>.

Second, a closer look at the species fluctuations revealed several striking patterns (Table 1). Peaks of picophytoplankton, nanophytoplankton and filamentous diatoms alternated with little or no overlap (Fig. 1d), and picophytoplankton and nanophytoplankton concentrations were negatively correlated (Table 1), indicative of competition between the phytoplankton groups. Predator–prey interactions could also be discerned. We found negative correlations of picophytoplankton with protozoa, and of nanophytoplankton both with rotifers and calanoid copepods (Table 1). This indicates that protozoa fed mainly on picophytoplankton, whereas rotifers and calanoid copepods fed mainly on larger nanophytoplankton, consistent with the structure of the food web (Fig. 1a). Conversely, the positive correlation of picophytoplankton with calanoid copepods may point at indirect mutualism between prey species and the predators of their competitors (that is, 'the enemy of my enemy is my friend'). Other striking patterns included the negative correlation between bacteria

<sup>1</sup>Aquatic Microbiology, Institute for Biodiversity and Ecosystem Dynamics, University of Amsterdam, Nieuwe Achtergracht 127, 1018 WS Amsterdam, the Netherlands. <sup>2</sup>Aquatic Ecology and Water Quality Management, University of Wageningen, Wageningen, the Netherlands. <sup>3</sup>Institute of Biosciences, University of Rostock, Rostock, Germany. <sup>4</sup>Ecology and Evolutionary Biology, Cornell University, Ithaca, New York 14853, USA. †Present address: Leibniz-Institute of Freshwater Ecology and Inland Fisheries, Alte Fischerhütte 2, 16775 Neuglobsow, Germany.

\*These authors contributed equally to this work.

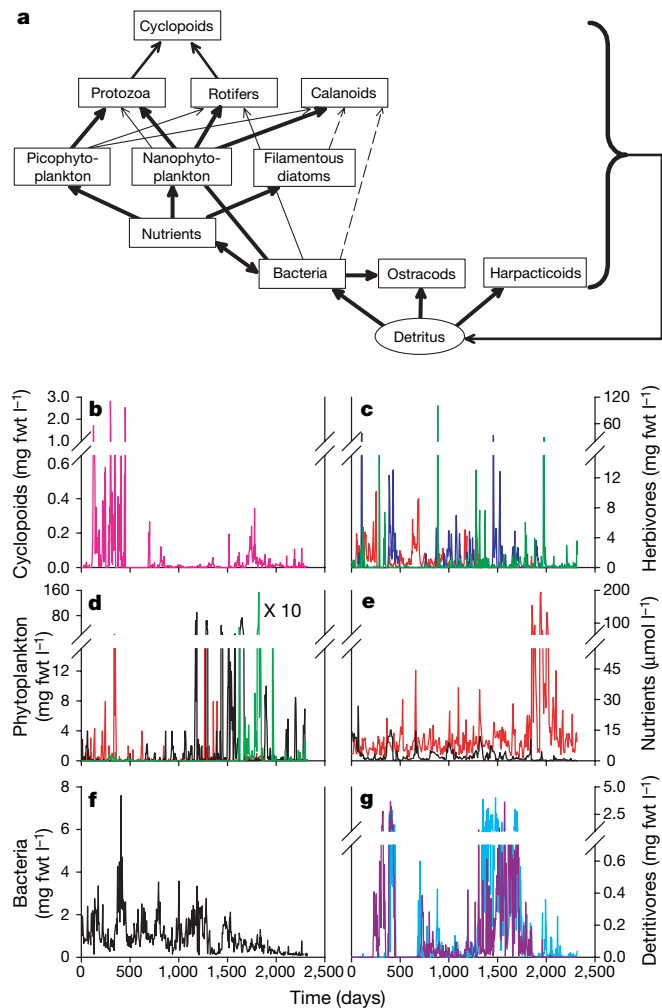


**Figure 1 | Description of the plankton community in the mesocosm experiment.** **a**, Food-web structure of the mesocosm experiment. The thickness of the arrows gives a first indication of the food preferences of the species, as derived from general knowledge of their biology. **b–g**, Time series of the functional groups in the food web (measured as freshwater biomass). **b**, Cyclopoid copepods; **c**, calanoid copepods (red), rotifers (blue) and protozoa (dark green); **d**, picophytoplankton (black), nanophytoplankton (red) and filamentous diatoms (green); note that the diatom biomass should be magnified by 10; **e**, dissolved inorganic nitrogen (red) and soluble reactive phosphorus (black); **f**, heterotrophic bacteria; **g**, harpacticoid copepods (violet) and ostracods (light blue).

and ostracods, and the positive correlation between bacteria and phosphorus. Although our interpretation of these correlation patterns is somewhat speculative, they correspond with the trophic links

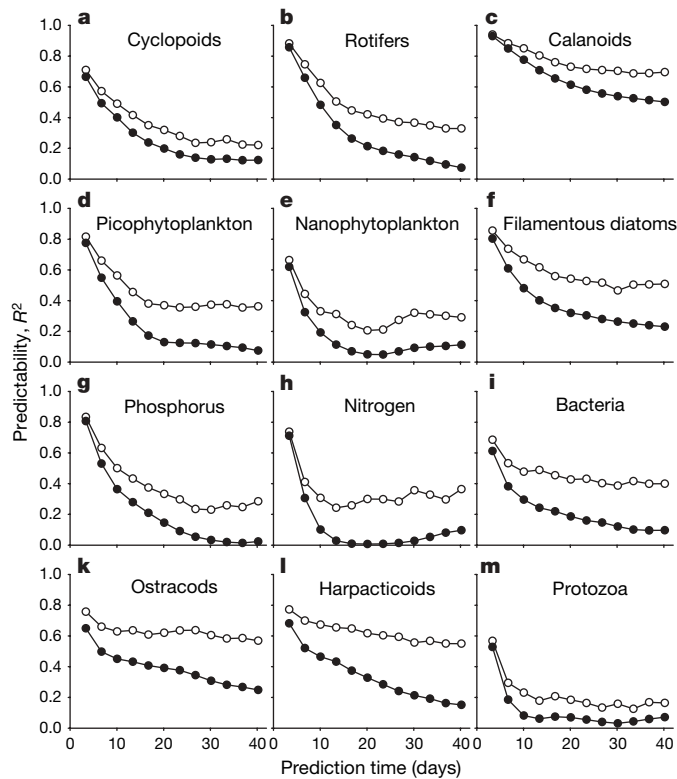


**Figure 2 | Predictability of the species decreases with increasing prediction time.** The predictability is quantified as the coefficient of determination  $R^2$  between predicted and observed data. Already after a few time steps, predictions by the nonlinear neural network model (open circles) were significantly better than predictions by the best-fitting linear model (filled circles) (see Supplementary Information for further details). **a**, Cyclopoid copepods; **b**, rotifers; **c**, calanoid copepods; **d**, picophytoplankton; **e**, nanophytoplankton; **f**, filamentous diatoms; **g**, soluble reactive phosphorus; **h**, dissolved inorganic nitrogen; **i**, bacteria; **k**, ostracods; **l**, harpacticoid copepods; **m**, protozoa.

in the food web. This shows that the observed fluctuations in species abundances were largely driven by species interactions in the food web, not by external forcing.

Third, we investigated the long-term predictability of the food-web dynamics. The predictability of a deterministic non-chaotic system with uncorrelated noise (for example, a limit cycle with sampling error) remains constant in time, whereas the predictability of chaotic systems decreases in time<sup>19</sup>. We fitted the time series to a neural network model<sup>20</sup> to generate predictions at different time intervals. For short-term forecasts of only a few days, most species had a high predictability of  $R^2 = 0.70–0.90$  (Fig. 2). However, the predictability of the species was much reduced when prediction times were

**Table 1 | Correlations between the species in the food web**

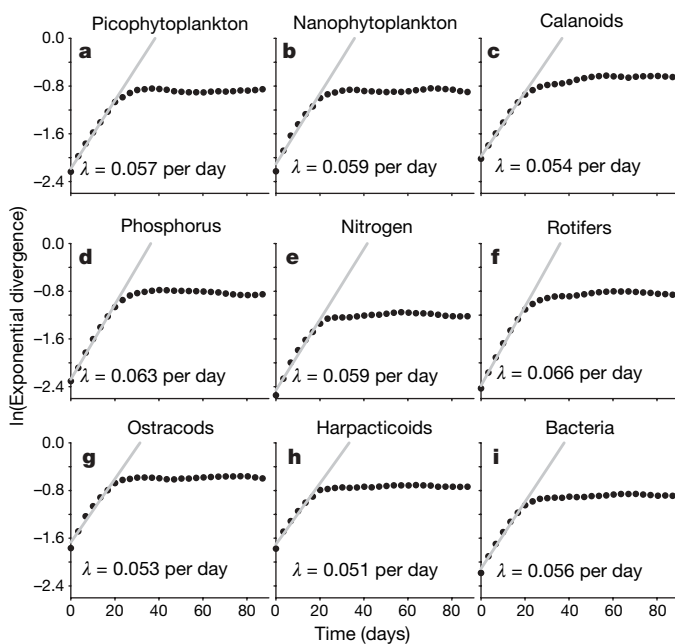
	Bacteria	Harpacticoid copepods	Ostracods	Nitrogen	Phosphorus	Picophytoplankton	Nanophytoplankton	Rotifers	Protozoa	Calanoid copepods
Bacteria	1	0.03	<b>-0.24***</b>	0.05	<b>0.19***</b>	0.03	<b>-0.17***</b>	<b>0.30***</b>	-0.17	<b>0.22***</b>
Harpacticoid copepods		1	<b>0.17**</b>	<b>-0.12*</b>	0.09	-0.04	-0.03	0.02	0.14	-0.04
Ostracods			1	<b>-0.16***</b>	-0.06	-0.04	0.01	-0.03	<b>0.19*</b>	-0.04
Nitrogen				1	0.08	-0.00	-0.02	-0.04	0.02	0.04
Phosphorus					1	-0.04	0.03	<b>0.10*</b>	-0.11	-0.09
Picophytoplankton						1	<b>-0.17***</b>	-0.03	<b>-0.22**</b>	<b>0.26***</b>
Nanophytoplankton							1	<b>-0.19***</b>	0.15	<b>-0.14*</b>
Rotifers								1	-0.02	-0.10
Protozoa									1	n.a.
Calanoid copepods										1

Table entries show the product-moment correlation coefficients, after transformation of the data to stationary time series (see Methods). Significance tests were corrected for multiple hypothesis testing by calculation of adjusted  $P$  values using the false discovery rate<sup>27</sup>. Significant correlations are indicated in bold: \*\*\* $P < 0.001$ ; \*\* $P < 0.01$ ; \* $P < 0.05$ ; n.a., not applicable. The correlation between calanoid copepods and protozoa could not be calculated, because their time series did not overlap. Filamentous diatoms and cyclopoid copepods were not included in the correlation analysis, because their time series contained too many zeros.

extended to 15–30 days. This is a characteristic feature of chaos, where short-term predictability is high, whereas the predictability decreases when making forecasts further into the future. However, decreasing predictability can also occur in linear (and therefore non-chaotic) systems exposed to stochastic perturbations. We therefore tested<sup>19</sup> whether the predictions of the nonlinear neural network model were significantly better than the predictions generated by the best-fitting linear model. Already after a few time steps, the nonlinear model yielded significantly higher predictabilities than the corresponding linear model for all species in the food web (Fig. 2; see Supplementary Information for the statistics). These findings demonstrate that (1) the predictability of the species abundances in the food web decreased in time, and (2) there was a strong nonlinear deterministic component in the food-web dynamics.

Fourth, we calculated the Lyapunov exponent, the hallmark of chaos in nonlinear systems. The dominant Lyapunov exponent  $\lambda$  is a measure of the rate of convergence or divergence of nearby trajectories<sup>21</sup>. Negative Lyapunov exponents indicate that nearby trajectories converge, which is representative of stable equilibria and periodic cycles. Conversely, positive Lyapunov exponents indicate divergence of nearby trajectories, which is representative of chaos. We used two different methods to calculate the Lyapunov exponent: a direct method and an indirect method.

The direct method started with a reconstruction of the attractor by time-delay embedding of each time series<sup>21–23</sup>. Exponential divergence (or convergence) of trajectories was calculated from nearby state vectors in the reconstructed state space<sup>24</sup>. The results show that the distance between initially nearby trajectories increased over time, and reached a plateau after about 20–30 days (Fig. 3). This matches the time horizon of 15–30 days obtained from the predictability estimates (Fig. 2). Lyapunov exponents were calculated from the initial slope of the exponential divergence, by using linear regression. This yielded significantly positive Lyapunov



**Figure 3 | Exponential divergence of the trajectories.** The Lyapunov exponent ( $\lambda$ ) is calculated as the initial slope of the ln-transformed exponential divergence versus time, as estimated by linear regression (grey line). All Lyapunov exponents were significantly different from zero (linear regression:  $P < 0.001$ ,  $n = 6$  or 7 depending on the species).

**a**, Picophytoplankton; **b**, nanophytoplankton; **c**, calanoid copepods; **d**, soluble reactive phosphorus; **e**, dissolved inorganic nitrogen; **f**, rotifers; **g**, ostracods; **h**, harpacticoid copepods; **i**, bacteria. Exponential divergence could not be calculated for filamentous diatoms, protozoa, and cyclopoid copepods, because their time series contained too many zeros.

exponents of strikingly similar value for all species (Fig. 3; mean  $\lambda \approx 0.057$  per day, s.d. = 0.005 per day,  $n = 9$ ). This gives much confidence that the species in the food web were all fully connected, and that their population dynamics were governed by the same chaotic attractor.

Direct methods cannot distinguish trajectory divergence caused by chaos from trajectory divergence due to noise<sup>9,20</sup>. Therefore, we also applied an indirect method, which calculates the Lyapunov exponent from a deterministic model. While indirect methods are not affected by noise, they rely on the assumption that the deterministic model provides an adequate representation of the system's deterministic skeleton. In our case, the model structure again followed the trophic structure of the food web (Fig. 1a). The model was used to calculate trajectory divergence at each time step by evaluation of the jacobian matrix (see Supplementary Information for details). This indirect method yielded a global Lyapunov exponent of  $\lambda = 0.04$  per day, characterizing the divergence of trajectories across the entire food web. We ran a bootstrap procedure based on 1,000 replicates to estimate the uncertainty of this value (see Supplementary Information). A one-sided confidence interval at the 95% confidence level yielded a lower bound of  $\lambda = 0.03$  per day. This confirmed that the Lyapunov exponent was significantly positive, and that this positive value was not due to noise.

In total, our analysis revealed several signatures of chaos. Despite constant external conditions, the food web showed strong fluctuations in species abundances that could be attributed to different species interactions. We found high predictability in the short term, reduced predictability in the long term, and significantly positive Lyapunov exponents. This shows that the population dynamics in the food web were characterized by exponential divergence of nearby trajectories, which provides the first experimental demonstration of chaos in a complex food web.

Compared with other systems, the time horizon for the predictability of our plankton community (15–30 days) is only slightly longer than the time horizon for the local weather forecast (about two weeks<sup>25</sup>). Lyapunov exponents were smaller in our plankton community ( $\lambda = 0.03$ – $0.07$  per day) than in recent experiments with microbial food webs<sup>11,12</sup> ( $\lambda = 0.08$ – $0.20$  per day). This might indicate that our plankton was 'less chaotic'. Alternatively, these differences in Lyapunov exponents might be attributed to differences in generation times, because most phytoplankton and zooplankton species in our experiment have longer generation times than the bacteria and ciliates used in these microbial food webs. Because the time horizon is inversely proportional to the Lyapunov exponent<sup>21</sup>, this suggests that the time horizon for the predictability of chaotic food webs scales with the generation times of the organisms involved.

Our findings have important implications for ecology and ecosystem management. First, our data illustrate that food webs can sustain strong fluctuations in species abundances for hundreds of generations. Apparently, stability is not required for the persistence of complex food webs. Second, non-equilibrium dynamics in food webs affect biodiversity and ecosystem functioning. For instance, fluctuations on timescales of 15–30 days, as observed in our experiment, offer a suitable range of temporal variability to promote species coexistence in plankton communities<sup>26</sup>. Hence, our results support the theoretical prediction that chaotic fluctuations generated by species interactions may contribute to the unexpected biodiversity of the plankton<sup>6</sup>, which provides a solution for one of the classic paradoxes in ecology known as the paradox of the plankton. Third, chaos limits the predictability of species abundances. In our experimental food web, predictability was lost on a timescale of 15–30 days, which corresponds to 5 to 15 plankton generations depending on the species. Because many other food webs have a similar structure of plants, herbivores, carnivores and a microbial loop, it is tempting to suggest that the observed loss of predictability in 5 to 15 generations is likely to apply to many other food webs as well.

## METHODS SUMMARY

The mesocosm consisted of a cylindrical plastic container (74 cm high, 45 cm diameter), which was filled with a 10 cm sediment layer and 90 l of water from the Baltic Sea. This inoculum provided all species in the food web. The mesocosm was maintained in the laboratory at a temperature of about 20 °C, a salinity of about 9‰, incident irradiation of 50 μmol photons m<sup>-2</sup> s<sup>-1</sup> (16:8 h light:dark cycle) and constant aeration. Species abundances were measured twice a week, whereas nutrients were measured weekly.

We interpolated each time series to obtain data with equidistant time intervals of 3.35 days. The interpolated time series were subsequently transformed to stationary time series with mean zero and standard deviation of 1. Long sequences of zero values were removed from the analysis.

We calculated the predictabilities of the species by fitting a neural network model to the time series, following ref. 20. For each species, the neural network predictions were based on the observed population abundances of the species itself and of those species with which it had a direct link in the food web (Fig. 1a).

We used two different methods to calculate the Lyapunov exponent. The direct method was based on attractor reconstruction by time-delay embedding of each time series<sup>23,24</sup>. We chose an embedding dimension of six and a time delay of one time step (see Supplementary Information). This direct method yielded Lyapunov exponents for each species separately. The consistency of these Lyapunov exponents provided an additional check on the robustness of our conclusions. The indirect method was based on a neural network approach to estimate the deterministic skeleton of the dynamics<sup>9,20</sup>. This deterministic skeleton was used to calculate one Lyapunov exponent characterizing the dynamics of the entire food web.

**Full Methods** and any associated references are available in the online version of the paper at [www.nature.com/nature](http://www.nature.com/nature).

Received 14 September; accepted 29 November 2007.

1. May, R. M. Biological populations with nonoverlapping generations: stable points, stable cycles, and chaos. *Science* **186**, 645–647 (1974).
2. May, R. M. Simple mathematical models with very complicated dynamics. *Nature* **261**, 459–467 (1976).
3. Gilpin, M. E. Spiral chaos in a predator–prey model. *Am. Nat.* **113**, 306–308 (1979).
4. Hastings, A. & Powell, T. Chaos in a three-species food chain. *Ecology* **72**, 896–903 (1991).
5. Vandermeer, J. Loose coupling of predator–prey cycles: entrainment, chaos, and intermittency in the classic MacArthur consumer–resource equations. *Am. Nat.* **141**, 687–716 (1993).
6. Huisman, J. & Weissing, F. J. Biodiversity of plankton by species oscillations and chaos. *Nature* **402**, 407–410 (1999).
7. Van Nes, E. H. & Scheffer, M. Large species shifts triggered by small forces. *Am. Nat.* **164**, 255–266 (2004).
8. Huisman, J., Pham Thi, N. N., Karl, D. M. & Sommeijer, B. Reduced mixing generates oscillations and chaos in the oceanic deep chlorophyll maximum. *Nature* **439**, 322–325 (2006).
9. Ellner, S. P. & Turchin, P. Chaos in a noisy world: new methods and evidence from time-series analysis. *Am. Nat.* **145**, 343–375 (1995).
10. Costantino, R. F., Desharnais, R. A., Cushing, J. M. & Dennis, B. Chaotic dynamics in an insect population. *Science* **275**, 389–391 (1997).

11. Becks, L., Hilker, F. M., Malchow, H., Jürgens, K. & Arndt, H. Experimental demonstration of chaos in a microbial food web. *Nature* **435**, 1226–1229 (2005).
12. Graham, D. W. *et al.* Experimental demonstration of chaotic instability in biological nitrification. *ISME J.* **1**, 385–393 (2007).
13. Zimmer, C. Life after chaos. *Science* **284**, 83–86 (1999).
14. McCann, K., Hastings, A. & Huxel, G. R. Weak trophic interactions and the balance of nature. *Nature* **395**, 794–798 (1998).
15. Neutel, A. M., Heesterbeek, J. A. P. & de Ruiter, P. C. Stability in real food webs: weak links in long loops. *Science* **296**, 1120–1123 (2002).
16. Heerkloss, R. & Klinkenberg, G. A long-term series of a planktonic foodweb: a case of chaotic dynamics. *Verh. Int. Verein. Theor. Angew. Limnol.* **26**, 1952–1956 (1998).
17. Scheffer, M. & Rinaldi, S. Minimal models of top-down control of phytoplankton. *Freshwat. Biol.* **45**, 265–283 (2000).
18. Fussmann, G. F., Ellner, S. P., Shertzer, K. W. & Hairston, N. G. Jr. Crossing the Hopf bifurcation in a live predator–prey system. *Science* **290**, 1358–1360 (2000).
19. Sugihara, G. & May, R. M. Nonlinear forecasting as a way of distinguishing chaos from measurement error in time series. *Nature* **344**, 734–741 (1990).
20. Nychka, D., Ellner, S., Gallant, A. R. & McCaffrey, D. Finding chaos in noisy systems. *J. R. Stat. Soc. B* **54**, 399–426 (1992).
21. Strogatz, S. H. *Nonlinear Dynamics and Chaos: With Applications to Physics, Biology, Chemistry, and Engineering* (Perseus, Cambridge, Massachusetts, 1994).
22. Takens, F. in *Dynamical Systems and Turbulence, Warwick 1980* (Lecture Notes in Mathematics vol. 898) (ed. Rand, D. A. & Young, L.S.) 366–381 (Springer, Berlin, 1981).
23. Kantz, H. & Schreiber, T. *Nonlinear Time Series Analysis* (Cambridge Univ. Press, Cambridge, UK, 1997).
24. Rosenstein, M. T., Collins, J. J. & De Luca, C. J. A practical method for calculating largest Lyapunov exponents from small data sets. *Physica D* **65**, 117–134 (1993).
25. Lorenz, E. N. Atmospheric predictability experiments with a large numerical model. *Tellus* **34**, 505–513 (1982).
26. Gaedeke, A. & Sommer, U. The influence of the frequency of periodic disturbances on the maintenance of phytoplankton diversity. *Oecologia* **71**, 25–28 (1986).
27. Benjamini, Y. & Hochberg, Y. Controlling the false discovery rate: a practical and powerful approach to multiple testing. *J. R. Stat. Soc. B* **57**, 289–300 (1995).

**Supplementary Information** is linked to the online version of the paper at [www.nature.com/nature](http://www.nature.com/nature).

**Acknowledgements** We thank W. Ebenhöf for suggestions on the experimental design, H. Albrecht, G. Hinrich, J. Rodhe, S. Stolle and B. Walter for help during the experiment, T. Huebener, I. Telesh, R. Schumann, M. Feike and G. Arlt for advice in taxonomic identification, and B. M. Bolker and V. Dakos for comments on the manuscript. The research of E.B., K.D.J. and J.H. was supported by the Earth and Life Sciences Foundation (ALW), which is subsidized by the Netherlands Organisation for Scientific Research (NWO). S.P.E.'s research was supported by a grant from the Andrew W. Mellon Foundation.

**Author Contributions** R.H. ran the experiment, counted the species and measured the nutrient concentrations. E.B., J.H., K.D.J., P.B. and S.P.E. performed the time series analysis. E.B., J.H., M.S. and S.P.E. wrote the manuscript. All authors discussed the results and commented on the manuscript.

**Author Information** Reprints and permissions information is available at [www.nature.com/reprints](http://www.nature.com/reprints). Correspondence and requests for materials should be addressed to J.H. ([jef.huisman@science.uva.nl](mailto:jef.huisman@science.uva.nl)).

## METHODS

**Experimental set-up.** The experiment<sup>16</sup> started on 31 March 1989, when the mesocosm was filled with a 10 cm sediment layer and 90 l of water from the Darss-Zingst estuary (southern Baltic Sea, 54° 26' N, 12° 42' E). Phytoplankton was divided in three functional groups: picophytoplankton consisting of 1–2 µm picocyanobacteria (mostly *Synechococcus* species); nanophytoplankton consisting of 3–5 µm eukaryotic flagellates (mainly *Rhodomonas lacustris* Pascher and Ruttner); and large filamentous diatoms (*Melosira moniliformis* (O.F.M.) C. Agardh). Herbivorous zooplankton was classified into three groups: protozoa (mainly large ciliates such as *Cyclidium* and *Strombidium* species); rotifers (mainly *Brachionus plicatilis* (O.F.M.)); and the calanoid copepod *Eurytemora affinis* (Poppe). Rotifers and protozoa were grazed by predators belonging to the cyclopoid copepods (unidentified species of the *Eucyclops* genus). The microbial loop was represented by heterotrophic bacteria and two groups of detritivores: ostracods and the harpacticoid copepod *Halectinosoma curticorne* (Boeck). Sampling of the mesocosm is described in Supplementary Information.

From 23 November 1990 to 5 March 1991, the length of the light period was temporarily reduced from 16 to 12 h per day. Accounting for a brief period of recovery, we therefore restricted our time series analysis to the period from 16 June 1991 onwards until the end of the experiment on 20 October 1997.

**Data treatment.** Several of our analyses required stationary time series, with equidistant data and homogeneous units of measurement. We therefore interpolated each time series by cubic hermite interpolation to obtain data with equidistant time intervals of 3.35 days. Nitrogen and phosphorus concentrations were transformed to equivalent units of 'biomass' assuming Redfield ratios<sup>28</sup>. Some functional groups remained below the detection limit for a long time, yielding long sequences of zero values. We shortened these time series by removing these long sequences of zero values. Also, the time series showed sharp ups and downs in species abundances. Therefore, all time series were re-scaled by a fourth-root power transformation. This power transformation homogenized the variances, and eliminated possible bias in the 'direct method' calculation of the Lyapunov exponents (see Supplementary Information). Subsequently, we removed long-term trends from the data by using a sliding window with a bandwidth of 300 days and a Gaussian kernel. Finally, the data were normalized by the transformation  $(x - \mu)/\sigma$ , where  $x$  is the original datapoint,  $\mu$  is the mean of the time series and  $\sigma$  is the standard deviation. Thus, we obtained stationary time series with mean zero and standard deviation of 1. The transformed time series are shown in the Supplementary Information.

**Predictability.** We developed a model to investigate the predictability of each species. Ideally, this model would be based on the biology of the species interactions. However, the exact mechanisms of species interaction in this food web are not known. For instance, we do not know the elemental stoichiometry of the different species, whether allelochemicals modified the species interactions, or whether zooplankton followed type II or type III functional responses. We may even lack information on some food-web components (for example, viruses were not measured). Using a mechanistically incorrect parametric model can lead to spurious results in nonlinear time series analysis<sup>29</sup>. Therefore, we used a semi-mechanistic approach in which the general model structure is based on biological knowledge about the food web, whereas non-parametric methods are used to fit aspects about which little is known.

In our case, we can exploit the food-web structure to make predictions. For each species, we used the following nonlinear model:

$$N_{i,t+T} = f_{i,T}(N_{i,t}, N_{1,t}, N_{2,t}, \dots, N_{m,t}) \quad (1)$$

Here,  $N_{i,t}$  is the population abundance (or nutrient concentration) of species  $i$  at time  $t$ ,  $T$  is the prediction time (that is, the number of days that we want to predict ahead), and  $f_{i,T}$  is an unknown function describing the change in the population abundance of focal species  $i$ . The function  $f_{i,T}$  uses the focal species  $i$ , and those species 1 to  $m$  that have a direct link in the food web to this focal species (Fig. 1a). For instance, predictions for picophytoplankton are based on picophytoplankton abundance, the nutrients nitrogen and phosphorus, and its herbivores (rotifers, protozoa and calanoid copepods) at the preceding time step. We estimated the unknown functions  $f_{i,T}$  by using the neural network algorithm of Nychka *et al.*<sup>20</sup> (see Supplementary Information for details).

We tested whether the nonlinear neural network model yielded significantly better predictions than the corresponding linear model. For this purpose, each nonlinear function  $f_{i,T}$  in equation (1) was replaced by a linear function of the same population abundances. The coefficients of this linear model were estimated by multiple regression. The significance test comparing the predictions of the linear and nonlinear model is explained in the Supplementary Information. **Lyapunov exponents.** We used direct and indirect methods (also called jacobian methods) to estimate Lyapunov exponents. Direct methods search the data for nearby pairs of state vectors. In other words, the time series are searched for pairs of data points at which all species abundances in the food web are in a similar state. The rate of trajectory divergence at subsequent times, averaged over many such pairs, is an estimate of the dominant Lyapunov exponent<sup>23,24</sup>. Because state vectors that are close in time are often also close in state space, temporal correlation in the data may obscure the divergence of trajectories. Our time series was sufficiently long to solve this problem by a Theiler window<sup>30</sup>, which is a moving window covering data before and after each data point (see Supplementary Information for details).

Jacobian methods are based on the development of a deterministic model of the underlying dynamics, called the 'deterministic skeleton'. The Lyapunov exponent is here calculated from the sequence of jacobian matrices of the deterministic skeleton, evaluated at the time series of observed or reconstructed state vectors<sup>9,20</sup>. Thus, jacobian methods require the preliminary step of estimating the deterministic skeleton. We estimated the deterministic skeleton by using a similar neural network model as for the predictability (equation (1)).

Both approaches have advantages and disadvantages. Direct methods cannot distinguish trajectory divergence caused by chaos from trajectory divergence caused by noise, and might therefore be less suitable for many ecological time series. Although our experimental system was maintained under controlled laboratory conditions, even small levels of environmental or demographic noise could bias direct methods towards positive estimates of the Lyapunov exponent. Jacobian methods are not biased by noise; their main problem is uncertainty in estimation of the deterministic skeleton. If the Lyapunov exponents obtained from both approaches are consistent, this adds further reliability to the results.

Further details on the calculation of Lyapunov exponents are provided in the Supplementary Information.

28. Redfield, A. C. The biological control of chemical factors in the environment. *Am. Sci.* **46**, 205–221 (1958).
29. Kendall, B. E. Cycles, chaos, and noise in predator–prey dynamics. *Chaos Solitons Fract.* **12**, 321–332 (2001).
30. Theiler, J. Spurious dimension from correlation algorithms applied to limited time-series data. *Phys. Rev. A* **34**, 2427–2432 (1986).